Food Hydrocolloids 156 (2024) 110262

Contents lists available at ScienceDirect

Food Hydrocolloids

journal homepage: www.elsevier.com/locate/foodhyd

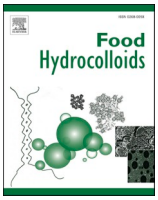

# Fabrication of zein/modified cyclodextrin nanofibers for the stability enhancement and delivery of curcumin

Yao Hu [a,b,**], Nicholas H. Rees [c], Chao Qiu [d], Jinpeng Wang [e], Zhengyu Jin [d], Ran Wang [a], Yinhua Zhu [a], Han Chen [a], Pengjie Wang [a], Siyuan Liu [a], Fazheng Ren [a], Gareth R. Williams [b,*]

[a] Department of Nutrition and Health, China Agricultural University, Beijing, 100193, China
[b] UCL School of Pharmacy, University College London, 29-39 Brunswick Square, London WC1N 1AX, UK
[c] Department of Chemistry, University of Oxford, Chemistry Research Laboratory, Mansfield Road, Oxford OX1 3TA, UK
[d] State Key Laboratory of Food Science and Resources, School of Food Science and Technology, Collaborative Innovation Center of Food Safety and Quality Control in Jiangsu Province, Jiangnan University, Wuxi, Jiangsu 214122, China
[e] Beijing Advanced Innovation Center for Food Nutrition and Human Health, China-Canada Joint Lab of Food Nutrition and Health (Beijing), School of Food and Health, Beijing Technology and Business University, 11 Fucheng Road, Beijing 100048, China

ARTICLE INFO

*Keywords:*
Curcumin
Electrospinning
Carboxylate cyclodextrin
Stability
Simulated digestion

ABSTRACT

Poor aqueous solubility and low stability are major problems which prevent curcumin exerting potent physiological activity. To overcome these challenges, this study fabricated zein-succinic acid modified cyclodextrin (SACD) nanofibers using the electrospinning technology. By optimising the proportion of SACD in the nanofibers, homogenous cylindrical fibers with a uniform size distribution could be obtained. The maximum loading capacity of the optimized nanofibers for curcumin was ca. 35.7 mg/g, as demonstrated by X-ray diffraction and differential scanning calorimetry. No cytotoxicity was observed for any of the Zein/SACD and curcumin-loaded Zein/SACD (Cur-Zein/SACD) nanofibers. The stability of curcumin in the Cur-Zein/SACD nanofibers was significantly improved (compared to the raw material) under conditions mimicking gastrointestinal environments and common heat sterilization processes. In a digestion study, less than 18% of the curcumin loading was released in simulated upper digestive tract conditions, suggesting most of the drug cargo should be able to reach the lower digestive tract and be utilized by the gut microbiota. This study suggests that Zein/SACD nanofibers could be a highly effective strategy for the encapsulation, stabilization and delivery of bioactive compounds, showing potential for food, pharmaceutical, and cosmetic products.

## 1. Introduction

Curcumin is a natural phenolic compound that shows antioxidant (Yuan et al., 2021), anti-inflammatory (Rafiee, Nejatian, Daeihamed, & Jafari, 2019), anticancer (Wu & Xue, 2020) and antibacterial (Yang et al., 2020) properties; thus, it has been widely explored in the fields of foods, pharmaceutics, and cosmetics. It is suggested that oral intake of curcumin could remodel the gut microenvironment of the colon, which might reduce challenges of colitis and colonic cancer (Shen & Ji, 2019). Notably, some curcumin metabolites generated by the gut microbiota in the colon were demonstrated to have superior biological activities in comparison to curcumin itself (Luca et al., 2020). However, it is difficult for curcumin to reach the colon and be utilized by the microbiota, due to its poor solubility in aqueous digestive media and its low chemical stability under environmental stresses (heat, salt, and alkaline conditions) experienced before arriving at the colon (Guo et al., 2020).

Researchers have attempted to solve these problems by constructing delivery systems for curcumin. A range of different carriers, including micro-/nano-particles (Peng et al., 2020; Xu et al., 2023), nanogels (Hu et al., 2021a), emulsions (Zhu et al., 2021), micelles (Zhi et al., 2021), and metal-organic frameworks (Qiu et al., 2020), have been reported to improve the chemical stability and bioavailability of compounds like curcumin. However, constructing these carriers usually requires complicated procedures, high cost, and/or results in a low loading capacity. For example, solubilizing curcumin in alkaline solution would cause some degradation during the preparation of a curcumin-loaded

* Corresponding author.
** Corresponding author.
*E-mail addresses:* huyao@cau.edu.cn (Y. Hu), g.williams@ucl.ac.uk (G.R. Williams).

https://doi.org/10.1016/j.foodhyd.2024.110262
Received 15 January 2024; Received in revised form 25 May 2024; Accepted 2 June 2024
Available online 4 June 2024

carrier (Peng et al., 2020). Carriers formed at low concentrations or with low yield lead to high cost (Hu et al., 2021a; Qiu et al., 2020). The preparation of electrospun nanofibers has advantages here due to the (i) ease of process implementation, (ii) ability to process a wide range of polymers, and (iii) control that can be exerted on the size, texture, and structure of the nanofibers (Topuz & Uyar, 2019). In addition, no additional procedures are required for the drying and purification of the products. Therefore, electrospinning has been widely explored for biomedical applications. While conceptually simple, there are some complexities in establishing the process successfully: the composition of the electrospinning solution (type of polymer, solvent used, concentration of polymer) and the processing parameters are crucial factors affecting the formation of fibers (Yu, Li, Williams, & Zhao, 2018).

Zein is an alcohol soluble protein extracted from corn with a molecular weight of typically about 40 kDa. It is rich in non-polar amino acids such as leucine, proline and alanine, which allow it to encapsulate hydrophobic molecules (Liu et al., 2022a). Moreover, zein has been identified as a promising material for protecting bioactive compounds from degradation in the upper digestive tract, and realizing targeted release in the colon (Tran, Duan, Lee, & Tran, 2019). Therefore, zein could be suitable to fabricate electrospun nanofibers with high loading efficiency for hydrophobic curcumin. The resultant fibers can be expected to stabilize the curcumin cargo in the upper digestive tract. By adjusting the composition of the spinning solvent and mixing with other polymers, the properties of zein-based fibers could be further improved (Deng et al., 2018). For instance, the storage and digestive stability of zein-based nanocarriers was found to be improved after coating with chitosan (Khan, Chen, & Liang, 2021). In this study, we seek to develop zein-based fibers to enhance the colon utilization of curcumin, by preventing release in gastric conditions, and protecting the curcumin from the mildly alkaline conditions found in the small intestine and other environmental stresses.

Cyclodextrins (CDs) comprise a series of aqueous-soluble oligosaccharides with a hydrophobic interior cavity and a hydrophilic exterior wall (Wankar et al., 2020), which have been widely explored to improve the solubility of poorly water-soluble drugs like curcumin (Arora, Saneja, & Jaglan, 2019). More importantly, it has been reported that CDs could interact with some of the amino acid residues of proteins (Hu, Jiang, et al., 2023), indicating CDs may have potential to regulate the properties of zein-based fibers. In our previous research, succinic acid-modified cyclodextrin (SACD) was obtained through a one-step dry-heating process (Hu, Qiu, et al., 2021). In comparison to unmodified CDs, the interactions of SACD with protein-derived components were much enhanced (Hu, Guo, et al., 2022; Hu, Xing, et al., 2023), and markedly increased water solubility (>250-fold greater) and encapsulation capacity for curcumin was observed (Hu, Qiu, et al., 2022). Based on these properties of SACD, it was hypothesized that SACD could interact with zein molecules and effectively alter the performance of zein-based nanofibers, enhancing encapsulation capacity.

In this study, the influence of SACD on the formation of zein-based electrospun nanofibers was explored. Fibers were prepared loaded with curcumin, and their cytotoxicity, stability and drug release behavior determined.

## 2. Materials and methods

### 2.1. Materials

Zein, β-CD (≥98%), curcumin (>99%), sodium hypophosphite (SHP), and PrestoBlue™ cell viability reagent were bought from Thermo Fisher Scientific (UK). Succinic acid (SA), pepsin from porcine gastric mucosa, pancreatin from porcine pancreas, bile bovine, and calcium chloride were purchased from Sigma-Aldrich (UK). Caco-2 cells were obtained from the American Type Culture Collection (UK). All other chemicals were of analytical grade. Deionized water was used for all experiments.

### 2.2. Preparation of SACD

SACD was prepared according to a previously reported method (Hu, Qiu, et al., 2021). Briefly, 4 g β-CD, 2.96 g SA, and 4 g SHP were mixed and dissolved in 40 mL of deionized water. After complete dissolution the mixture was poured into a 15 cm crystallizing dish, which was then transferred to an oven at 100 °C and held for 5 h to evaporate all the water from the sample. The modification process was conducted by placing the dried mixture into a 140 °C oven for 20 min to obtain the crude product, followed by dissolution in 20 mL deionized water and precipitation in 200 mL absolute ethanol. The final SACD product was prepared by washing the precipitant with absolute ethanol 2–3 times, then drying at 50 °C overnight.

### 2.3. Preparation of zein/SACD nanofibers

To prepare zein/SACD nanofibers, working solutions for electrospinning were firstly prepared. SACD was dissolved in 2 mL of 90% aqueous acetic acid at a range of concentrations (0, 3, 6, 9, 12, 15, 18, and 21% w/v), followed by adding zein into the solution to give a zein concentration of 35% (w/v). The working solution was obtained after 12 h of dissolution with continuous stirring, then transferred into a plastic syringe fitted with a 20G precision tip (Nordson EFD, UK). Afterwards, the syringe was loaded onto a syringe pump (78–9100C, Cole Parmer, UK), and the needle was connected to a high-voltage direct-current power supply (HCP 35–35,000, FuG Elektronik, Germany). Baking paper was used to cover a metal plate collector connected to the grounded electrode. The electrospinning process was conducted at 15 kV (environmental conditions: 20 ± 2 °C, relative humidity 40 ± 5%), the distance from the needle tip to the collector was set at 10 cm, and the flow rate was 1 mL/min.

### 2.4. Curcumin-loaded zein/SACD (Cur-Zein/SACD) nanofibers

The preparation of Cur-Zein/SACD nanofibers was analogous to the zein/15% SACD system, except that curcumin was added into the working solution to give a final concentration of 0.5, 1, 2, 3, 5, and 8% (w/v). To determine the curcumin content in the carriers, 2 mg of Cur-Zein/SACD nanofibers were dissolved in 1 mL of 90% aqueous acetic acid solution and the absorbance measured at 429 nm on a Cary UV–visible spectrophotometer (Agilent, USA). The encapsulation efficiency (EE) of curcumin in the nanofibers was then calculated using equation (1)

$$\mathrm{EE}\ (\%) = \frac{\text{Measured amount of curcumin in Cur} - \text{Zein/SACD nanofibers}}{\text{Initial amount of curcumin added to the spinning solution}} \times 100\% \quad (1)$$

### 2.5. Electrospinning solution characterization

Viscosity was measured with a AR1500ex rheometer (TA Instruments, USA) with a 40 mm plate geometry at constant shear rate of 100 $s^{-1}$. The electrical conductivity was measured using a conductivity meter (DDS-11 A, INESA, China) at 25 °C. The surface tension was recorded using the pendant-drop method with a OCA25 Zcontact angle measurement system (DataPhysics Instruments, Germany).

### 2.6. Morphological charateristics

A PhenomPro benchtop scanning electron microscope (SEM; ThermoFisher, Netherlands) was used to acquire images. Samples were deposited on carbon tape and coated with gold before analysis. After acquiring SEM images, the mean diameter of the nanofibers was calculated from 100 points using the ImageJ software (National Institutes of Health, USA).

### 2.7. X-ray diffraction (XRD)

XRD data were obtained using a MiniFlex 600 X-ray diffractometer (Rigaku, Japan) supplied with Cu Kα radiation. The experiment was conducted over the 2θ range of 4–40°, the voltage and current were 40 kV and 15 mA, and the scan speed was set as 3° $min^{-1}$.

### 2.8. Differential scanning calorimetry (DSC)

DSC was performed on a Q2000 DSC instrument (TA Instruments, USA). Approximately 3 mg of sample was weighed and sealed in Tzero aluminium pans with non-hermetic lids. The samples were heated from 30 to 200 °C at 10 °C/min, under a nitrogen atmosphere.

### 2.9. Fourier transform infrared (FTIR) spectroscopy

FTIR spectra of the prepared samples were collected using a Spectrum 100 spectrometer (PerkinElmer, USA). Data were collected over the wavenumber range 400–4000 $cm^{-1}$ at a resolution of 1 $cm^{-1}$.

### 2.10. NMR spectroscopy

An Avance III 400 MHz NMR spectrometer (Bruker, USA) was used to collect solution $^{13}C$ NMR spectra. Solid state NMR (SSNMR) spectra were obtained on a Bruker Avance AVIII HD 400 MHz spectrometer. Samples were packed in 4 mm O.D. rotors. $^{13}C$ CPMAS spectra were acquired with a spinning speed of 10 kHz, a contact time of 1.5 ms, recycling delay of 1.5 s, and 20,000 scans. Spectra were externally referenced to the CO signal of α-glycine at 176.5 ppm (relative to δ TMS at 0 ppm).

### 2.11. Cytotoxicity

The cytotoxicity of the nanofibers was assessed using Caco-2 cells (passage number of 39) according to a literature method (Dziemidowicz, Brocchini, & Williams, 2021). Briefly, 1 mg of a fiber sample was placed into each well of a 96-well plate. For the control group, pure curcumin was dissolved in DMSO as stock solution, then 9 μL of the stock solution (containing the same amount of curcumin as loaded in the fibers) was added into the 96-well plate. The plate was covered with a lid and sterilized under UV light for 30 min. Cells were precultured in Dulbecco's modified Eagle medium (DMEM; Gibco™, Life Technologies, UK) supplemented with penicillin–streptomycin solution (1% v/v) and 20% v/v heat-inactivated fetal bovine serum (Gibco™, Life Technologies, UK). Before the cytotoxicity assay, cells were suspended at a concentration of $5 \times 10^4$ viable cells/mL. 150 μL of the cell suspension was added into each well of the plate. An untreated cells control was also established and the plate was incubated at 37 °C for 48 h. After the incubation, the nanofiber pieces were removed, and the PrestoBlue™ reagent added. Viability was determined following the manufacturer instructions. The assay was conducted in triplicate on different batches (three independent experiments), and three replicates were carried out for each batch.

### 2.12. Stability of Cur-Zein/SACD nanofibers

The stability of curcumin in Cur-Zein/SACD nanofibers was evaluated according to our previously reported method (Hu, Qiu, et al., 2022) with some modifications. The physiological stability was assessed by incubating 2 mg of the fibers in 5 mL of media at the gastric pH (pH = 2, room temperature), small intestinal pH (pH = 7.4, room temperature), physiological salt concentration (0.9% NaCl in water, room temperature), and physiological temperature (37 °C). The pasteurization stability of curcumin loaded in Zein/SACD nanofibers was determined by suspending 2 mg of the samples in 5 mL of deionized water and incubating at 65 °C for 30 min. Similarly, the sample suspension was incubated at 121 °C for 30 min to evaluate the stability of Cur-Zein/SACD nanofibers under high temperature steam sterilization conditions. After the above treatments, the remaining curcumin in the nanofibers was extracted using 1 mL of 90% aqueous acetic acid solution and quantified using a Cary UV–visible spectrophotometer (AgilentUSA) at 429 nm. The retention index (RI) was then calculated using equation (2) to quantify the stability of curcumin in the fibers.

$$\text{RI}\ (\%) = \frac{\text{Remaining amount of curcumin after treatment}}{\text{Initial amount of curcumin present}} \times 100\% \quad (2)$$

### 2.13. Release of curcumin

The release behavior of curcumin from the nanofibers was determined using a standard INFOGEST *in vitro* digestion model including gastric and small intestinal stages, based on the protocol of Brodkorb et al. (2019). The gastric fluid was constructed with simulated gastric electrolytes and pepsin, while the small intestinal fluid consisted of simulated small intestinal electrolytes, bile, and pancreatin. Both of the gastric and small intestinal fluids were preincubated at 37 °C before use. For the release test, 10 mg of sample was added into 5 mL of gastric fluid and incubated at 37 °C for 2 h. At the end of the gastric stage, 100 μL of the solution was removed for analysis, while the remaining fluid was mixed with 5 mL of small intestinal fluid, followed by adjusting the pH to 7 using 5 M NaOH. After incubating at 37 °C for another 2 h, 100 μL of the solution was removed. The curcumin released from the nanofibers at different digestive stages was quantified using a UV–vis spectrophotometer at 429 nm.

### 2.14. Statistical analysis

All measurements were repeated in triplicate. Numeric results are displayed as mean ± standard deviation. ANOVA analysis (followed by a post-hoc LSD test) of the experimental data was carried out using the SPSS 20 statistical software (SPSS Inc., USA). Differences were considered at a significance level of 95% ($p < 0.05$).

## 3. Results and discussion

### 3.1. Preparation of SACD

The molecular structure of SACD was assessed by FTIR and $^{13}C$ NMR. As shown in Fig. S1 (Supporting Information), a new peak relating to the C═O ester bond in SACD could be observed at 1724 $cm^{-1}$ in the FTIR spectrum, indicating esterification had occurred successfully between the β-CD and SA molecules. The $^{13}C$ NMR spectrum of SACD shows the appearance of a new C═O signal, arising from the presence of succinate groups, at 173.18 ppm (Fig. S2) and a characteristic peak at 18.20 ppm

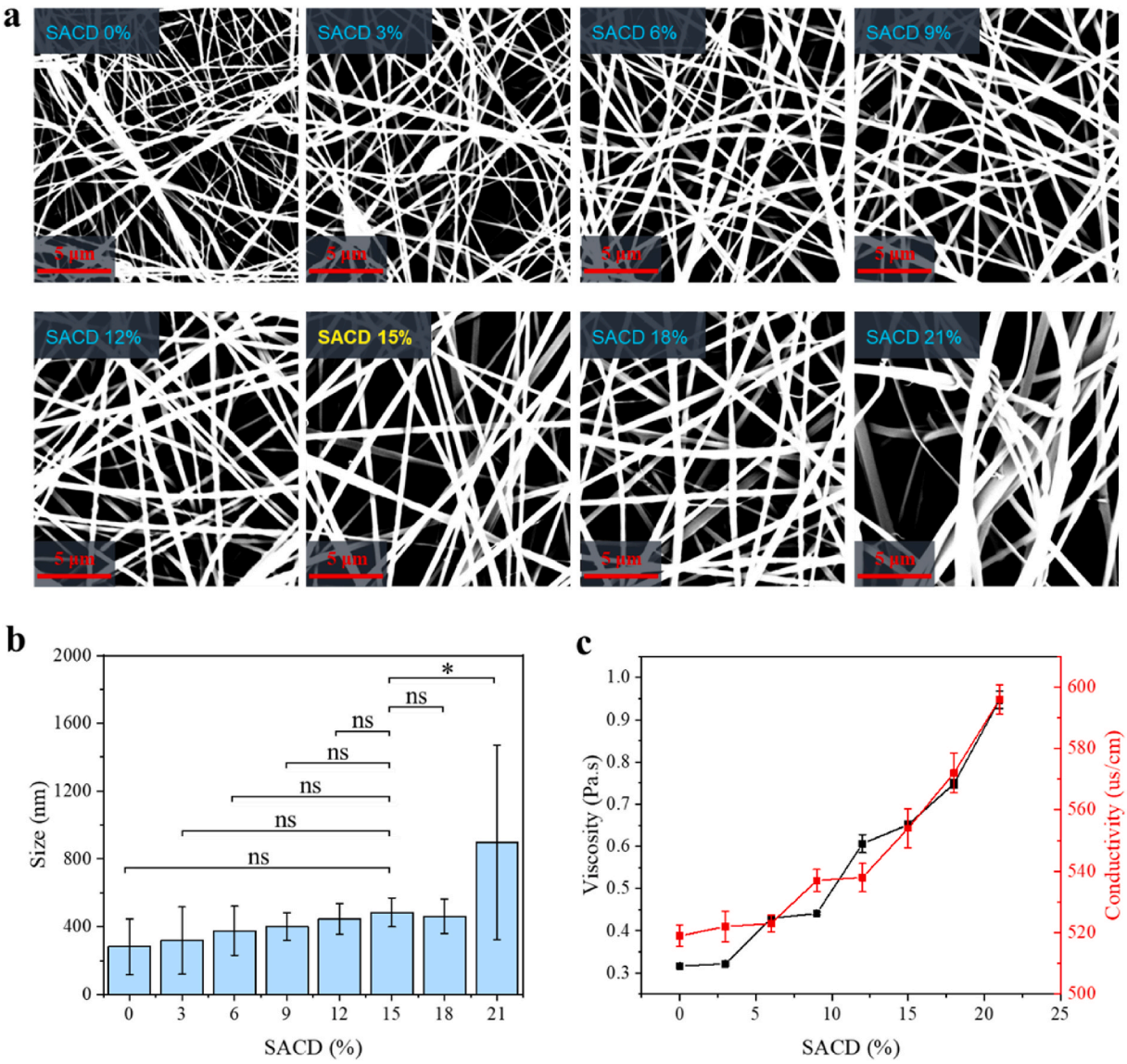


**Fig. 1.** SEM images (a) and fiber diameters (b) of Zein/SACD nanofibers with different proportions of SACD (0–21%, w/v) loaded in the electrospinning solution, and the viscosity and conductivity of the electrospinning solutions at different SACD proportions (c).

related to the ester bond. These features are not observed in the spectrum of β-CD (Fig. S2), and are consistent with $^{13}C$ NMR spectra of SACD obtained in a previous study (Hu, Qiu, et al., 2021). Therefore, it could be confirmed that SACD was prepared successfully, as reported previously (Hu, Qiu, et al., 2021).

### 3.2. Morphology of Zein/SACD nanofibers

SEM micrographs of Zein/SACD nanofibers prepared with different SACD concentrations are displayed in Fig. 1a, and a summary of the diameters is given in Fig. 1b. It can be seen that the pure zein fibers (SACD 0%) have non-homogenous size and curved morphology. The morphology of the Zein/SACD nanofibers became notably more cylindrical and the fiber diameter more homogenous as the proportion of SACD in the electrospinning solution rose from 0% to 15% w/v. The viscosity and conductivity of the electrospinning solution increased with rising SACD proportions (Fig. 1c), while no significant change was observed in the surface tension values (Table S1). According to Moradkhannejhad, Abdouss, Nikfarjam, Mazinani, and Heydari (2018) and Song, Yao, and Li (2010), combining zein with other biomolecules can contribute to increased electrical conductivity of the electrospinning solution. The addition of additional SACD solute as its concentration increases will also increase the viscosity of the solution. The addition of SACD could improve the electrospinnability of zein-based solutions by both of these mechanisms. This leads to increased size uniformity of the Zein/SACD nanofibers with the addition of SACD.

As the SACD proportion further increased to 18–21%, adhesion and entangling phenomena appeared, along with the formation of coarse fibers (Fig. 1a). The diameter distribution of the Zein/SACD nanofibers at 18% SACD became wider, with both narrower and thicker fibers present, and the fibers also displayed a tendency to curl, contributing to reduced homogeneity. This phenomenon of homogeneity loss was further aggravated when the SACD proportion in the electrospinning solutions increased to 21%. A similar trend was reported by Aman Mohammadi et al. (2021), who found that an excessive proportion of polylactic acid in zein-based electrospinning solutions contributed to the formation of coarse fibers due to enhanced molecular entanglements in the solution. Fig. 1c reveals high electrical conductivity of the Zein/-SACD solution at high SACD levels (18% and 21%), which could contribute to reduced spinnability of the solutions (Facchi, Souza, Almeida, Bonafé, & Martins, 2021). Based on the observed cylindrical morphology and narrow fiber diameter distribution, the SACD

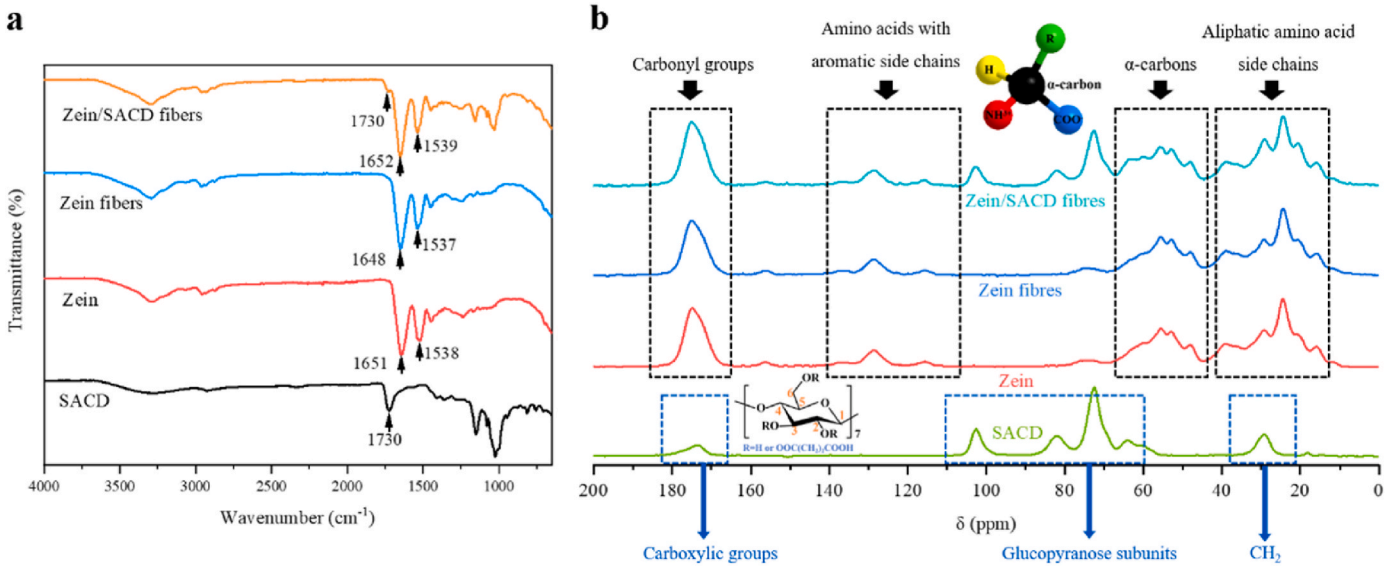


**Fig. 2.** FTIR (a) and solid-state $^{13}C$ NMR spectra (b) of zein, SACD, zein nanofibers, and Zein/15% SACD nanofibers.

concentration in the electrospinning solution was fixed at 15% w/v for further experiments.

### 3.3. Characterization of Zein/SACD nanofibers

The FTIR spectra of zein, SACD, and Zein/15% SACD nanofibers are presented in Fig. 2a, and provide information the intermolecular interactions in the Zein/SACD nanofibers. The characteristic peak of SACD at 1730 $cm^{-1}$ is related to the stretching vibration of the ester C═O group, while peaks displayed at 3294, 2925, 1155 $cm^{-1}$ and 1027 $cm^{-1}$ correspond to the stretching vibrations of *O*–H, $CH_2$, *C*–*O*–C, and *C*–OH, respectively. The characteristic band of zein at 3295 $cm^{-1}$ is attributed to *O*–H and *N*–H stretching, while C═O stretching (amide I) and *N*–H bending (amide II) appear at 1651 $cm^{-1}$ and 1538 $cm^{-1}$, respectively (Sun et al., 2020). Considering the spectra of the nanofibers, the zein peak at 3295 $cm^{-1}$ is present in both without significant movement. However, the zein amide I peak moves from 1651 $cm^{-1}$ to 1648 $cm^{-1}$ after electrospinning, and then shifts back to 1652 $cm^{-1}$ when introducing SACD into the electrospinning solution. According to Zhang et al. (2023), a shift of the zein band at 3295 $cm^{-1}$ is related to the formation of intermolecular hydrogen bonds, while peak shifts at 1651 $cm^{-1}$ correspond to intermolecular electrostatic interactions (Sun et al., 2020). The above results indicate that the interactions between SACD and zein are dominated by electrostatics.

In order to further elucidate the electrostatic interactions between zein and SACD molecules in the nanofibers, solid-state $^{13}C$ NMR spectra were obtained. As shown in Fig. 2b, the peak of zein at 175 ppm corresponds to carbonyl (C═O) carbon, and peaks in the range of 140–100 ppm are related to the side chains of aromatic amino acids. Resonances at 70-45 ppm are related to α-carbon atoms (connecting the amino group, carboxyl group, and the side chain group), while peaks in the 45-15 ppm range correspond to aliphatic amino acid side chains (Bicudo, Forato, Batista, & Colnago, 2005; Neo et al., 2014). The characteristic peaks of SACD at 173.75 ppm and 29.19 ppm are related to carbonyl (C═O) and methylene ($CH_2$) groups, respectively. The peaks at 102.59 ppm, 82.00 ppm, 72.50 ppm and 64.03 ppm correspond to C-1, C-4 and C-5, C-3 and C-2 and C-6 of glucopyranose subunits on the molecular framework of CD.

After forming Zein/SACD nanofibers, the peaks of both zein and SACD are still visible in the spectra, mostly at the same positions as in the starting materials. However, the C-6 of SACD, where the succinic acid groups most likely grafted, shifted from 64.03 ppm to higher field by 0.84 ppm. The characteristic peaks associated with succinic acid in SACD molecules were masked by zein, but peaks associated with the zein amino acid side chain (128.02 ppm and 15.84 ppm) move to lower field by 0.42 ppm and 0.17 ppm after electrospinning, indicating that there were electrostatic interactions between SACD and the zein side chains. The characteristic peaks of SACD related to intermolecular hydrogen bonding did not shift significantly, indicating that this was not extensive in the Zein/SACD nanofibers, as also suggested by IR spectroscopy. Alcantara et al. (2020) observed that the characteristic peak of zein at 172.5 ppm shifted slightly to lower field after electrostatic interactions taking place between zein and positively charged layered double hydroxide particles, and it appears our results are consistent with the development of electrostatic interactions in the fibers.

### 3.4. Morphology of Cur-Zein/SACD nanofibers

A series of curcumin-loaded fibers was prepared using solutions containing 35% w/v zein and 15% w/v SACD. We first sought to optimise the curcumin loading. Adding an excess amount of curcumin could result in phase separation of the pure drug from the Zein/SACD nanofibers, and a literature study (de Oliveira Mori et al., 2014) reported large beads and thicker fibers were observed after introducing large amounts of tannin into the electrospun nanofibers of zein. Thus, we prepared a family of materials with different drug loadings.

Fig. 3 displays SEM images of fibers fabricated with a range of curcumin concentrations (Fig. 3a) as well as a summary of their diameters (Fig. 3b). Similar cylindrical morphological properties and sizes are found with curcumin concentrations of 0.5–2% (w/v) in the electrospinning solution, while large beads and thick fibers formed when the curcumin concentration was higher than 2%. The viscosity of the Cur-Zein/SACD electrospinning solutions increased from 0.65 Pa s to 0.83 Pa s as the curcumin concentration rose from 0% to 2%, while a decrease of viscosity was observed at values > 2% (Fig. 3c). The electrical conductivity of the solutions declined as the concentration varied from 0 to 6% curcumin and then rose slightly. No significant differences were observed between the surface tension of the Cur-Zein/SACD solutions (Table S2). It was thus confirmed that the viscosity of the Cur-Zein/SACD electrospinning solutions was the main influencing factor regulating the formation and morphology of the prepared nanofibers, with the optimal fibers obtained at the highest viscosity.

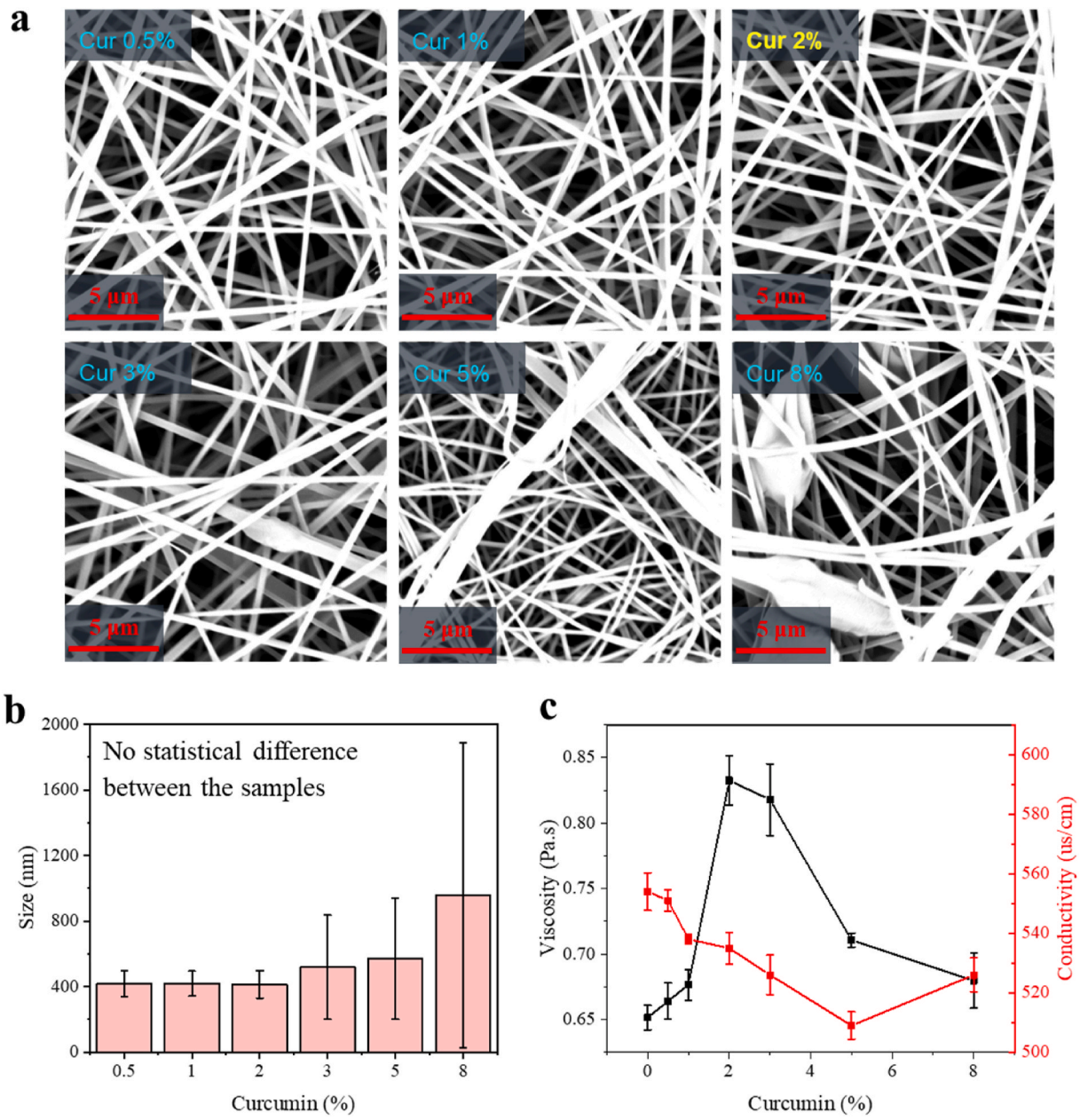


**Fig. 3.** SEM images (a) and fiber diameters (b) of Cur-Zein/SACD nanofibers prepared with different curcumin loading in the electrospinning solution, and the viscosity and conductivity of the electrospinning solutions (c).

### 3.5. Physical form

According to Fig. 4a, curcumin has a highly ordered crystalline structure, with many Bragg reflections visible in the XRD pattern, while blank Zein/SACD nanofibers have an amorphous structure, with only broad haloes present. When curcumin was loaded in the Zein/SACD fibers, no obvious Bragg reflections were observed when curcumin levels in the electrospinning solution were below 2%, indicating that the drug was amorphously dispersed in the fibers and/or the amount of any crystalline material present was below the detection limit of the instrument. When the curcumin level in the electrospinning solution exceeded 2%, obvious curcumin reflections at 2θ of 8.8° are visible and the intensity of these increases with concentration, indicating the existence of curcumin crystals in the nanofibers. It is suggested that the encapsulation of curcumin in the nanofibers reached saturation at 2%, and concentrations above this led to the presence of an excess amount of curcumin which recrystallized during the electrospinning process. These results are consistent with the viscosity date for the Cur-Zein/SACD solutions: the viscosity decreasing at high curcumin concentrations (>2%) could be attributed to the precipitation of curcumin crystals.

DSC analysis was conducted to verify the findings of XRD. As shown in Fig. 4b, pure curcumin has a sharp melting peak at 178 °C, corresponding to the reported melting point (Marcolino, Zanin, Durrant, Benassi, & Matioli, 2011). Zein/SACD nanofibers displayed a broad peak at low temperatures relating to water loss, and a wide thermal denaturation peak at ca. 175 °C, with enthalpy of 3.401 J/g. These observations confirm the crystallinity of curcumin and the amorphous nature of the Zein/SACD nanofibers. When 0.5–2% curcumin was added into the Zein/SACD electrospinning solution, the melting peak of curcumin is absent, and no significant changes in the endotherm centered at ca. 175 °C were observed. This indicates that there was no crystallized curcumin in the nanofibers. However, when the curcumin level in the electrospinning solution reached 3–8%, the enthalpy of the endotherm at 175 °C increased significantly (Table S3). The contribution to this

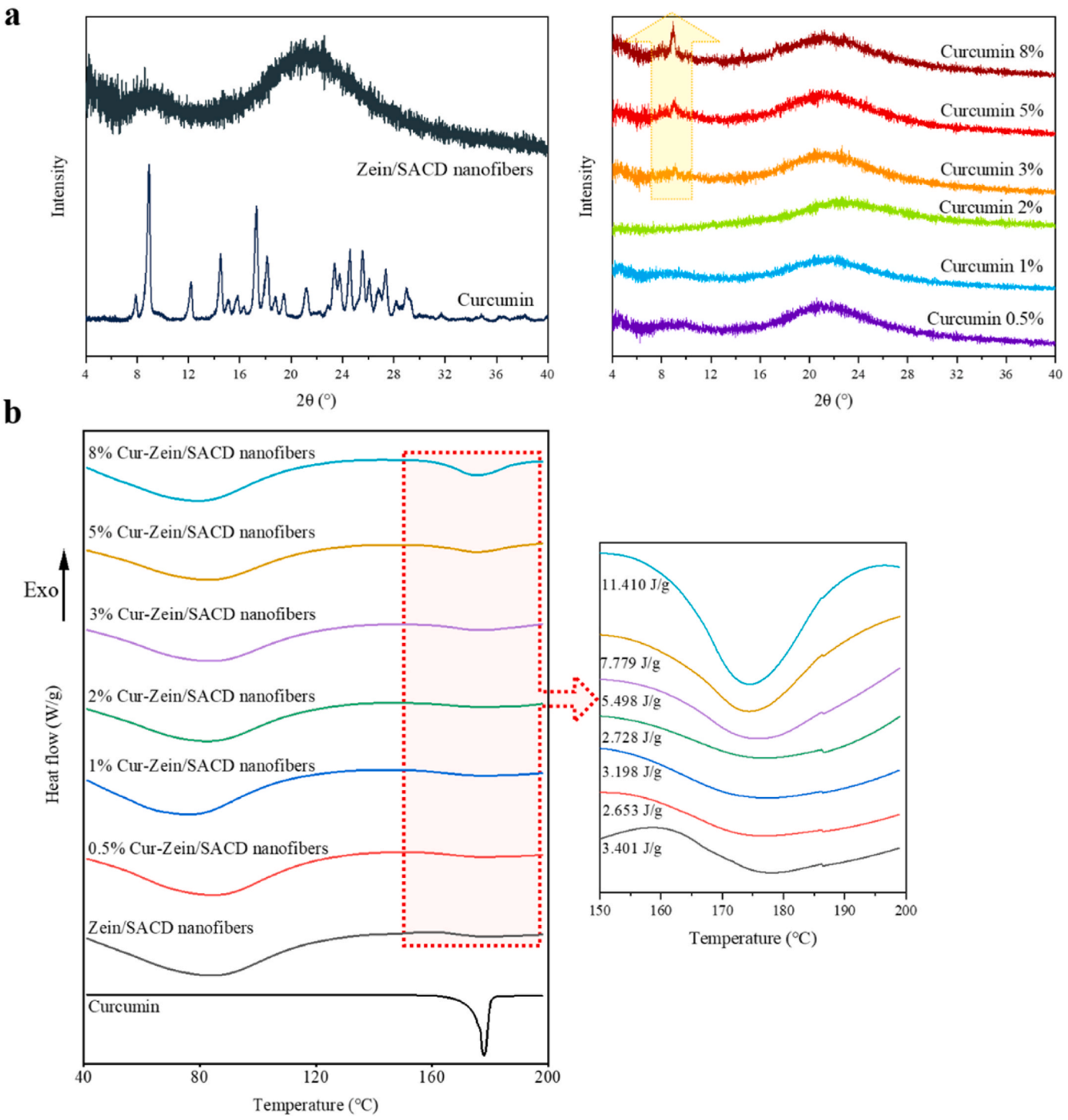


**Fig. 4.** The XRD patterns (a) and DSC curves (b) of curcumin, Zein/SACD nanofibers, and Cur-Zein/SACD nanofibers.

endotherm from the zein is constant, and thus the additional enthalpy must be caused by the presence of crystalline curcumin. Hence, these results agree with the XRD data and suggest excess curcumin formed crystals in the nanofiber matrix.

These results, together with those from XRD and SEM, confirm that the maximum addition of curcumin in the electrospinning solution should be below 2% w/v. At a 2% w/v curcumin concentration, the encapsulation efficiency (EE) was found to be 92.7% (Table S3). This corresponds to a w/w concentration of 35.7 mg/g in the Cur-Zein/SACD nanofibers. Compared with the Cur-SACD inclusion complexes prepared in our previous study, the loading capacity of curcumin here is increased by 3.57 times (Hu, Qiu, et al., 2022). The maximum EE% (99.6%) is obtained using a 1% w/v solution, corresponding to a w/w concentration of 19.5 mg/g in the Cur-Zein/SACD nanofibers. Hence, unless otherwise specified, Cur-Zein/SACD nanofibers prepared with a 1% w/v curcumin solution were used in subsequent research. Solid-state $^{13}C$ NMR spectra of these fibers are presented in Fig. S3. Clear chemical shifts could be observed for groups belong to both SACD and zein in the Cur-Zein/SACD nanofibers, indicating that curcumin interacts with both the SACD cavities and the zein molecules.

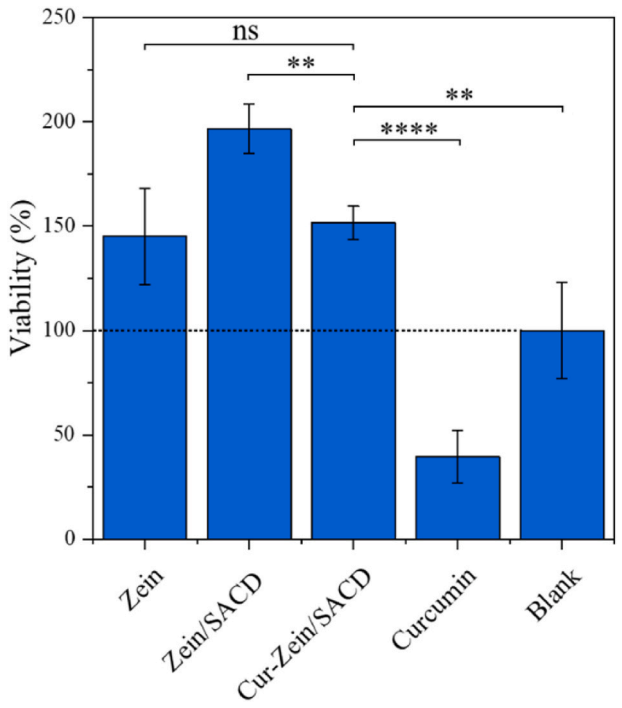


**Fig. 5.** The viability of Caco-2 cells treated with zein, Zein/SACD nanofibers, Cur-Zein/SACD nanofibers, and curcumin, together with an untreated cells control ("Blank"). ns" indicates no significant difference and $p > 0.05$, while significant differences are denoted as $^{**}p < 0.01$ and $^{****}p < 0.0001$.

### 3.6. Cytotoxicity

The cytotoxicity of the Zein/SACD nanofibers and Cur-Zein/SACD nanofibers was evaluated using Caco-2 cells as model intestinal epithelial cells. As can be seen from Fig. 5, after co-incubation with zein, the viability of Caco-2 cells was significantly higher than that of the blank control group, indicating that zein may promote cell proliferation and act as a source of nutrition. Caco-2 cells incubated with Zein/SACD nanofibers showed still higher cell viability. According to Lin, Li, Zhao, Hu, and Zhang (2012), high surface hydrophobicity limits the role of zein nanofibers in promoting cell proliferation. After using collagen to improve the hydrophilicity for the surface of zein nanofibers, Lin observed significantly improved cell proliferation. Therefore, it is believed that here the interaction of SACD with zein could also improve the surface hydrophilicity, making the Zein/SACD fibers more conducive to cell proliferation.

The viability of Caco-2 cells incubated with Cur-Zein/SACD nanofibers decreased in comparison to the Zein/SACD nanofibers, but was still higher than that of the untreated cells. Notably, pure curcumin showed significant cytotoxicity to Caco-2 cells. These data show the cytocompatibility of both Zein/SACD and Cur-Zein/SACD nanofibers, and also indicates that Zein/SACD fibers can avoid undesired interactions between curcumin and intestinal epithelial cells. The Zein/SACD nanofibers hence have the potential to be used as delivery carriers of bioactive compounds.

### 3.7. Stability of curcumin in Cur-Zein/SACD nanofibers

After the ingestion of Cur-Zein/SACD nanofibers, it is important for the curcumin in the nanofibers to remain stable before its release and absorption, to ensure high bioavailability. The stability of curcumin in Cur-Zein/SACD nanofibers was thus investigated under gastrointestinal

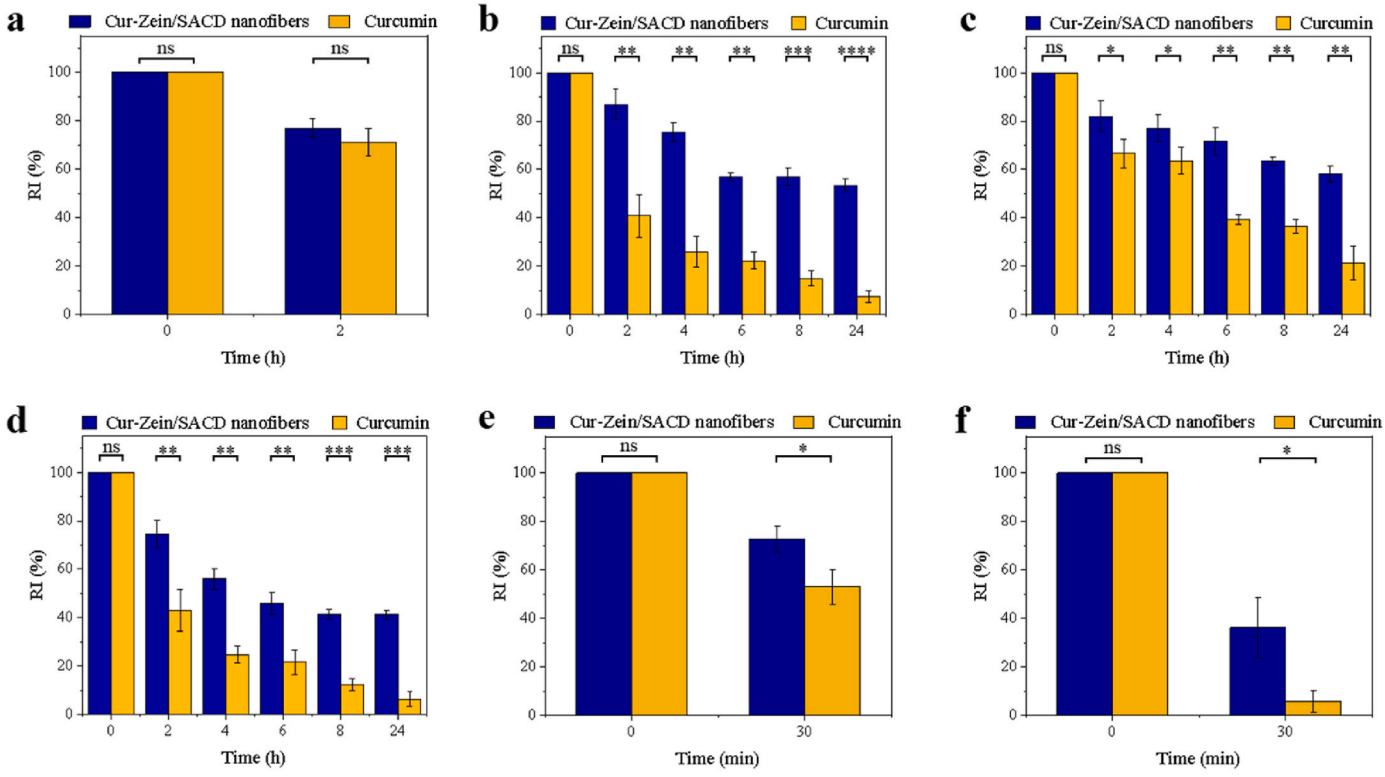


**Fig. 6.** The RI of curcumin in Cur-Zein/SACD nanofibers after immersion in media with gastric pH (pH = 2, aqueous HCl) (a), small intestinal pH (pH = 7.4, PBS) (b), physiological salt concentration (0.9% sodium chloride in water) (c), physiological temperature (37 °C in water) (d), pasteurization (65 °C in water) (e), and high temperature steam sterilization (121 °C in water) (f). "ns" indicates no significant difference and $p > 0.05$; significance is denoted as $^{**}p < 0.01$, $^{***}p < 0.001$, $^{****}p < 0.0001$.

conditions including gastric pH, intestinal pH, physiological salt concentration and physiological temperature. As presented in Fig. 6a, after treatment under gastric pH, there was reduction in the RI of curcumin both with the free drug and Cur-Zein/SACD nanofibers. These were not significantly different, with a drop in concentration after 2 h of immersion but RI higher than 70%. Under treatment at the small intestine pH (pH = 7.4) the RI of free curcumin decreased continuously with the treatment time, until only 7.4 ± 2.6 % remained after 24 h. In contrast, 53.3 ± 2.7% of the curcumin remained from the Cur-Zein/SACD nanofibers after 24 h (Fig. 6b). It is known that curcumin become less stable under neutral to alkaline conditions because of deprotonation taking place (Kharat, Du, Zhang, & McClements, 2017; Liu et al., 2018). The results indicate that the interactions between curcumin and the fiber matrix (both zein and SACD molecules), prevented the degradation of curcumin under neutral to alkaline conditions. Similar findings of diminished curcumin degradation were reported by Wang, Leung, Kee, and English (2010) when interactions between curcumin and ionic surfactants took place in micelles or vesicles.

Fig. 6c shows the RI of curcumin treated with physiological salt concentration (0.9% NaCl at room temperature). The results showed that the RI of curcumin in Cur-Zein/SACD nanofibers was 58.1 ± 3.1% after 24 h, while the RI of free curcumin was only 21.2 ± 7.1% after this period of time. Similarly, curcumin in the Cur-Zein/SACD nanofibers was more stable than free curcumin after treatment at physiological temperature (37 °C in deionized water), with an RI value of 41.3 ± 1.9% after 24 h, cf. 6.2 ± 3.0% for free curcumin (Fig. 6d). In comparison to typical physiological salt concentrations, the mild heat treatment of the body temperature appears to be a more significant factor for the degradation of curcumin during the digestion process. This is consistent with previous results of Hu, Qiu, et al. (2022). These findings indicate that Cur-Zein/SACD nanofibers could be excellent delivery systems for curcumin, able to protect it from degradation in physiological microenvironments.

In addition, heat treatments commonly applied during food processing could have a significant influence on the stability of curcumin molecules. Such procedures include pasteurization and high temperature steam sterilization treatments. After pasteurization, 53.1 ± 7.2% of free curcumin remained intact, while the RI of curcumin in the Cur-Zein/SACD nanofibers was 72.9 ± 5.3% (Fig. 6e). More curcumin loss was observed under high temperature steam sterilization, with only 5.7 ± 4.6% left in the free curcumin sample after treatment and 36.2 ± 12.6% from the Cur-Zein/SACD nanofibers (Fig. 6f). As the temperature increased, more curcumin loss was observed for both free curcumin and curcumin encapsulated in the fibers. Begum, Chutia, Bora, Deb, and Mahanta (2024) reported a similar tendency of decreased curcumin retention in emulsions after treating at higher temperatures. Though more curcumin loss was observed under a more intense heating condition, the fibers clearly protect the curcumin loading to at least some extent.

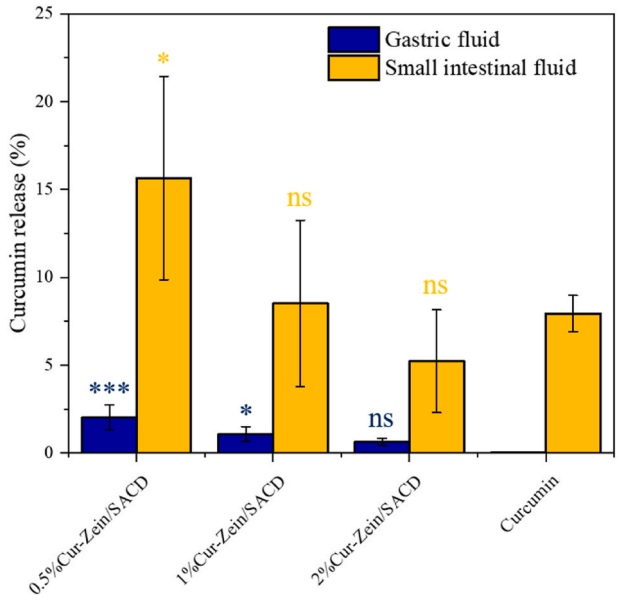


**Fig. 7.** The release of curcumin from Cur-Zein/SACD nanofibers in an *in vitro* simulated digestion model. "ns" indicates no significant difference compared to the pure curcumin group ($p > 0.05$), while significance is denoted as * $p < 0.05$, *** $p < 0.001$.

### 3.8. Release of curcumin from Cur-Zein/SACD nanofibers

The INFOGEST *in vitro* digestion model was used to evaluate curcumin release during the digestion process. Samples with different loading (0.5%, 1%, and 2% curcumin in the electrospinning solution) were investigated to explore the effect of curcumin loading on the release behavior. As can be seen from Fig. 7, after 2 h almost no curcumin in free form is dissolved in the gastric fluid due to its hydrophobic nature. The average release of curcumin from the 0.5%Cur-Zein/SACD nanofibers in gastric fluid was 2%, suggesting that only a small amount of curcumin on the surface of the fibers was released. When the loading is increased, the mean curcumin release in the gastric phase decreased to 1.1 ± 0.4% and 0.7 ± 0.2% for 1%Cur-Zein/SACD and 2%Cur-Zein/SACD nanofibers, respectively. Similar findings were observed in the small intestine phase, where the release from the Cur-Zein/SACD nanofibers after 2 h decreased from 15.7 ± 5.8% to 5.2 ± 2.9% with an increase of curcumin loading.

It can be observed that the amount of curcumin released in the small intestinal stage was significantly higher than that in the gastric stage. This could be attributed to the intrinsic solubility of zein being higher at the small intestinal pH, which is above the isoelectric point of zein (Komijani, Mohebbi, & Ghorani, 2022). Additionally, the existence of bile in the simulated small intestinal fluid can help solubilize hydrophobic molecules by forming bile salt micelles (Wright, Pietrangelo, & MacNaughton, 2008). In comparison to the gastric phase, it is much easier for loosely bound curcumin at the surface of Cur-Zein/SACD fibers to be dissolved into solution under the action of bile and other components.

Although the proportion of the curcumin cargo released in both gastric and small intestinal fluids decreased with rising curcumin loading levels in the fibers, the absolute amount of curcumin released from the fibers increased (from $2.0 \times 10^{-3}$ mg to $2.5 \times 10^{-3}$ mg in the gastric phase, and from $15.5 \times 10^{-3}$ mg to $20.1 \times 10^{-3}$ mg in the small intestinal phase). It can be speculated that loosely bound curcumin molecules in the fibers tend to release into the digestive fluids attribute to the solubilizing effect of bile salts and partial dissolution of zein. The decreased curcumin release percentage with rising curcumin loading suggests that a higher proportion of curcumin molecules were tightly bound to the matrix of the fibers at higher loading.

According to Kamguyan et al. (2022), zein is not easily degraded by pepsin in the gastric fluid or trypsin in the small intestinal fluid, so it can be an effective material to use to improve the stability and limit the release of curcumin in the upper digestive tract. It is reported that zein could be partially degraded by trypsin near its isoelectric point, but its enzymolysis in the small intestine can be effectively inhibited when it is combined with polysaccharides containing ionic groups (Liu, Yang, Chen, & Cheng, 2022). Bisharat et al. (2019) prepared acetylated homoamylose/zein composite films to make a slow-release formulation of paracetamol, and found that the film coating effectively delayed the release of the drug during digestion, with less than 15% released into the digestive fluid after 6 h of gastric and small intestinal-simulating digestion. The results above indicate that combining the carboxylated SACD with zein could be an efficient strategy for reducing the release and enhancing the stability of curcumin in the upper digestive tract.

Generally, bioactive guest molecules that are not released from a

carrier after upper gastrointestinal digestion will be transferred to the lower digestive tract, and fermented by the gut microbiota in the colon (Hu, Lin, et al., 2023). The physiological activity of drugs absorbed in the lower digestive tract is significantly different from that in the upper digestive tract due to a number of bioactive metabolites forming during colonic fermentation, which could confer benefits to human health (Williamson, Kay, & Crozier, 2018). Though zein is relatively resistant to digestive enzyme hydrolysis in the upper digestive tract, it is reported to be susceptible to degradation by the action of colonic microbes (Wang, Zhang, Zhu, Jiang, & Zhang, 2018). Therefore, loading curcumin in Zein/SACD nanofibers could be a promising strategy to target the release of curcumin to the lower digestive tract. More work should be conducted in the future to study the digestive behavior of the Cur-Zein/SACD nanofibers in the lower digestive tract, and the corresponding physiological activities.

## 4. Conclusions

Improving the stability and achieving targeted release of curcumin is crucial to allow it to fulfil all its potential bioactive functions. In this study, Zein/SACD nanofibers were fabricated by electrospinning. The introduction of SACD to the zein system significantly improved the properties of the resultant nanofibers, with Zein/SACD formulations having straighter fibers, smoother surfaces, fewer beads, and more uniform size distributions. Electrostatic interactions between SACD and the amino acid side chains of zein were identified by IR and NMR spectroscopies. A family of fibers containing varying loadings of curcumin was then generated. The loading capacity of Zein/SACD nanofibers for curcumin was found to be 35.7 mg/g. Cytocompatibility tests demonstrated that both Zein/SACD nanofibers and Cur-Zein/SACD nanofibers were nontoxic. Compared to the free drug, the stability of curcumin in Cur-Zein/SACD nanofibers was significantly improved under conditions reminiscent of gastrointestinal environments and common heat sterilization processes. *In vitro* simulated digestion results showed that only 5.9–15.7% of curcumin was released from the Cur-Zein/SACD nanofibers in the upper digestive tract, suggesting that the fibers can be used as delivery carriers to give targeted release of curcumin in the lower digestive tract. Future research will further assess the release of curcumin from Cur-Zein/SACD nanofibers using *in vivo* digestion models.

## CRediT authorship contribution statement

**Yao Hu:** Writing – review & editing, Writing – original draft, Validation, Methodology, Investigation, Funding acquisition, Formal analysis, Data curation, Conceptualization. **Nicholas H. Rees:** Writing – review & editing, Resources, Methodology, Investigation, Data curation. **Chao Qiu:** Supervision, Methodology, Conceptualization. **Jinpeng Wang:** Supervision, Funding acquisition. **Zhengyu Jin:** Supervision, Funding acquisition, Conceptualization. **Ran Wang:** Formal analysis. **Yinhua Zhu:** Visualization. **Han Chen:** Formal analysis. **Pengjie Wang:** Visualization. **Siyuan Liu:** Writing – original draft, Funding acquisition. **Fazheng Ren:** Supervision, Funding acquisition. **Gareth R. Williams:** Writing – review & editing, Supervision, Resources, Project administration, Methodology, Funding acquisition, Conceptualization.

## Declaration of competing interest

The authors declare that they have no known competing financial interests or personal relationships that could have appeared to influence the work reported in this paper.

## Data availability

Data will be made available on request.

## Acknowledgements

This work was supported by National Key R&D Program of China (2021YFD2101000/2021YFD2101003), China Scholarship Council (202106760040), and the Fellowship of China National Postdoctoral Program for Innovative Talents (BX20230416).

## Appendix A. Supplementary data

Supplementary data to this article can be found online at https://doi.org/10.1016/j.foodhyd.2024.110262.

## References

Alcântara, A. C. S., Darder, M., Aranda, P., & Ruiz-Hitzky, E. (2020). Zein-layered hydroxide biohybrids: Strategies of synthesis and characterization. *Materials, 13*(4), 825.

Aman Mohammadi, M., Ramezani, S., Hosseini, H., Mortazavian, A. M., Hosseini, S. M., & Ghorbani, M. (2021). Electrospun antibacterial and antioxidant zein/polylactic acid/hydroxypropyl methylcellulose nanofibers as an active food packaging system. *Food and Bioprocess Technology, 14*(8), 1529–1541.

Arora, D., Saneja, A., & Jaglan, S. (2019). Cyclodextrin-based delivery systems for dietary pharmaceuticals. *Environmental Chemistry Letters, 17*(3), 1263–1270.

Begum, F., Chutia, H., Bora, M., Deb, P., & Mahanta, C. L. (2024). Characterization of coconut milk waste nanocellulose based curcumin-enriched Pickering nanoemulsion and its application in a blended beverage of defatted coconut milk and pineapple juice. *International Journal of Biological Macromolecules, 259*, Article 129305.

Bicudo, T. C., Forato, L. A., Batista, L. A. R., & Colnago, L. A. (2005). Study of the conformation of γ-zeins in purified maize protein bodies by FTIR and NMR spectroscopy. *Analytical and Bioanalytical Chemistry, 383*(2), 291–296.

Bisharat, L., Barker, S. A., Narbad, A., & Craig, D. Q. M. (2019). In vitro drug release from acetylated high amylose starch-zein films for oral colon-specific drug delivery. *International Journal of Pharmaceutics, 556*, 311–319.

Brodkorb, A., Egger, L., Alminger, M., Alvito, P., Assunção, R., Ballance, S., et al. (2019). INFOGEST static in vitro simulation of gastrointestinal food digestion. *Nature Protocols, 14*(4), 991–1014.

de Oliveira Mori, C. L. S., dos Passos, N. A., Oliveira, J. E., Mattoso, L. H. C., Mori, F. A., Carvalho, A. G., et al. (2014). Electrospinning of zein/tannin bio-nanofibers. *Industrial Crops and Products, 52*, 298–304.

Deng, L., Zhang, X., Li, Y., Que, F., Kang, X., Liu, Y., et al. (2018). Characterization of gelatin/zein nanofibers by hybrid electrospinning. *Food Hydrocolloids, 75*, 72–80.

Dziemidowicz, K., Brocchini, S., & Williams, G. R. (2021). A simple route to functionalising electrospun polymer scaffolds with surface biomolecules. *International Journal of Pharmaceutics, 597*, Article 120231.

Facchi, D. P., Souza, P. R., Almeida, V. C., Bonafé, E. G., & Martins, A. F. (2021). Optimizing the Ecovio® and Ecovio®/zein solution parameters to achieve electrospinnability and provide thin fibers. *Journal of Molecular Liquids, 321*, Article 114476.

Guo, Q., Su, J., Shu, X., Yuan, F., Mao, L., Liu, J., et al. (2020). Production and characterization of pea protein isolate-pectin complexes for delivery of curcumin: Effect of esterified degree of pectin. *Food Hydrocolloids, 105*, Article 105777.

Hu, G., Batool, Z., Cai, Z., Liu, Y., Ma, M., Sheng, L., et al. (2021a). Production of self-assembling acylated ovalbumin nanogels as stable delivery vehicles for curcumin. *Food Chemistry, 355*, Article 129635.

Hu, Y., Guo, C., Lin, Q., Hu, J., Li, X., Sang, S., et al. (2022b). Complexation of curcumin with cyclodextrins adjusts its binding to plasma proteins. *Food & Function, 13*(17), 8920–8929.

Hu, Y., Jiang, L., Xing, K., Li, X., Sang, S., McClements, D. J., et al. (2023a). Cyclodextrins promoting the analysis and application of food-grade protein/peptides. *Trends in Food Science & Technology, 137*, 63–73.

Hu, Y., Lin, Q., Zhao, H., Li, X., Sang, S., McClements, D. J., et al. (2023c). Bioaccessibility and bioavailability of phytochemicals: Influencing factors, improvements, and evaluations. *Food Hydrocolloids, 135*, Article 108165.

Hu, Y., Qiu, C., Julian McClements, D., Qin, Y., Long, J., Jiao, A., et al. (2022a). Encapsulation, protection, and delivery of curcumin using succinylated-cyclodextrin systems with strong resistance to environmental and physiological stimuli. *Food Chemistry, 376*, Article 131869.

Hu, Y., Qiu, C., McClements, D. J., Qin, Y., Fan, L., Xu, X., et al. (2021b). Simple strategy preparing cyclodextrin carboxylate as a highly effective carrier for bioactive compounds. *Journal of Agricultural and Food Chemistry, 69*(37), 11006–11014.

Hu, Y., Xing, K., Li, X., Sang, S., McClements, D. J., Chen, L., et al. (2023b). Cyclodextrin carboxylate improves the stability and activity of nisin in a wider range of application conditions. *Npj Science of Food, 7*(1), 20.

Kamguyan, K., Kjeldsen, R. B., Moghaddam, S. Z., Nielsen, M. R., Thormann, E., Zór, K., et al. (2022). Bioadhesive tannic-acid-functionalized zein coating achieves engineered colonic delivery of ibd therapeutics via reservoir microdevices. *Pharmaceutics, 14*(11), 2536.

Khan, M. A., Chen, L., & Liang, L. (2021). Improvement in storage stability and resveratrol retention by fabrication of hollow zein-chitosan composite particles. *Food Hydrocolloids, 113*, Article 106477.

Kharat, M., Du, Z., Zhang, G., & McClements, D. J. (2017). Physical and chemical stability of curcumin in aqueous solutions and emulsions: Impact of ph, temperature,

and molecular environment. *Journal of Agricultural and Food Chemistry, 65*(8), 1525–1532.
Komijani, M., Mohebbi, M., & Ghorani, B. (2022). Assembly of electrospun tri-layered nanofibrous structure of zein/basil seed gum/zein for increasing the bioaccessibility of lycopene. *LWT–Food Science and Technology, 161*.
Lin, J., Li, C., Zhao, Y., Hu, J., & Zhang, L.-M. (2012). Co-electrospun nanofibrous membranes of collagen and zein for wound healing. *ACS Applied Materials & Interfaces, 4*(2), 1050–1057.
Liu, J., Lei, L., Ye, F., Zhou, Y., Younis, H. G. R., & Zhao, G. (2018). Aggregates of octenylsuccinate oat β-glucan as novel capsules to stabilize curcumin over food processing, storage and digestive fluids and to enhance its bioavailability. *Food & Function, 9*(1), 491–501.
Liu, J., Li, Y., Zhang, H., Liu, S., Yang, M., Cui, M., et al. (2022a). Fabrication, characterization and functional attributes of zein-egg white derived peptides (EWDP)-chitosan ternary nanoparticles for encapsulation of curcumin: Role of EWDP. *Food Chemistry, 372*, Article 131266.
Liu, L., Yang, S., Chen, F., & Cheng, K.-W. (2022b). Polysaccharide-zein composite nanoparticles for enhancing cellular uptake and oral bioavailability of curcumin: Characterization, anti-colorectal cancer effect, and pharmacokinetics. *Frontiers in Nutrition, 9*.
Luca, S. V., Macovei, I., Bujor, A., Miron, A., Skalicka-Woźniak, K., Aprotosoaie, A. C., et al. (2020). Bioactivity of dietary polyphenols: The role of metabolites. *Critical Reviews in Food Science and Nutrition, 60*(4), 626–659.
Marcolino, V. A., Zanin, G. M., Durrant, L. R., Benassi, M. D. T., & Matioli, G. (2011). Interaction of curcumin and bixin with β-cyclodextrin: Complexation methods, stability, and applications in food. *Journal of Agricultural and Food Chemistry, 59*(7), Article 3348e3357.
Moradkhannejhad, L., Abdouss, M., Nikfarjam, N., Mazinani, S., & Heydari, V. (2018). Electrospinning of zein/propolis nanofibers; antimicrobial properties and morphology investigation. *Journal of Materials Science: Materials in Medicine, 29*(11).
Neo, Y. P., Perera, C. O., Nieuwoudt, M. K., Zujovic, Z., Jin, J., Ray, S., et al. (2014). Influence of heat curing on structure and physicochemical properties of phenolic acid loaded proteinaceous electrospun fibers. *Journal of Agricultural and Food Chemistry, 62*(22), 5163–5172.
Peng, S., Zhou, L., Cai, Q., Zou, L., Liu, C., Liu, W., et al. (2020). Utilization of biopolymers to stabilize curcumin nanoparticles prepared by the pH-shift method: Caseinate, whey protein, soy protein and gum Arabic. *Food Hydrocolloids, 107*, Article 105963.
Qiu, C., Julian McClements, D., Jin, Z., Qin, Y., Hu, Y., Xu, X., et al. (2020). Resveratrol-loaded core-shell nanostructured delivery systems: Cyclodextrin-based metal-organic nanocapsules prepared by ionic gelation. *Food Chemistry, 317*, Article 126328.
Rafiee, Z., Nejatian, M., Daeihamed, M., & Jafari, S. M. (2019). Application of different nanocarriers for encapsulation of curcumin. *Critical Reviews in Food Science and Nutrition, 59*(21), 3468–3497.
Shen, L., & Ji, H. F. (2019). Bidirectional interactions between dietary curcumin and gut microbiota. *Critical Reviews in Food Science and Nutrition, 59*(18), 2896–2902.
Song, T.-y., Yao, C., & Li, X.-s. (2010). Electrospinning of zein/chitosan composite fibrous membranes. *Chinese Journal of Polymer Science, 28*(2), 171–179.
Sun, X., Pan, C., Ying, Z., Yu, D., Duan, X., Huang, F., et al. (2020). Stabilization of zein nanoparticles with k-carrageenan and tween 80 for encapsulation of curcumin. *International Journal of Biological Macromolecules, 146*, 549–559.
Topuz, F., & Uyar, T. (2019). Electrospinning of cyclodextrin functional nanofibers for drug delivery applications. *Pharmaceutics, 11*(1), 6.
Tran, P. H. L., Duan, W., Lee, B. J., & Tran, T. T. D. (2019). Drug stabilization in the gastrointestinal tract and potential applications in the colonic delivery of oral zein-based formulations. *International Journal of Pharmaceutics, 569*, Article 118614.
Wang, Z., Leung, M. H. M., Kee, T. W., & English, D. S. (2010). The role of charge in the surfactant-assisted stabilization of the natural product curcumin. *Langmuir, 26*(8), 5520–5526.
Wang, H., Zhang, X., Zhu, W., Jiang, Y., & Zhang, Z. (2018). Self-assembly of zein-based microcarrier system for colon-targeted oral drug delivery. *Industrial & Engineering Chemistry Research, 57*(38), 12689–12699.
Wankar, J., Kotla, N. G., Gera, S., Rasala, S., Pandit, A., & Rochev, Y. A. (2020). Recent advances in host-guest self-assembled cyclodextrin carriers: Implications for responsive drug delivery and biomedical engineering. *Advanced Functional Materials, 30*, 1909049.
Williamson, G., Kay, C. D., & Crozier, A. (2018). The bioavailability, transport, and bioactivity of dietary flavonoids: A review from a historical perspective. *Comprehensive Reviews in Food Science and Food Safety, 17*, 1054–1112.
Wright, A. J., Pietrangelo, C., & MacNaughton, A. (2008). Influence of simulated upper intestinal parameters on the efficiency of beta carotene micellarisation using an in vitro model of digestion. *Food Chemistry, 107*(3), 1253–1260.
Wu, W., & Xue, W. (2020). Evaluation of anticancer activity of honokiol by complexation with hydroxypropyl-β-cyclodextrin. *Colloids and Surfaces B: Biointerfaces, 196*, Article 111298.
Xu, H., Li, J., McClements, D. J., Cheng, H., Long, J., Peng, X., et al. (2023). Eggshell waste act as multifunctional fillers overcoming the restrictions of starch-based films. *International Journal of Biological Macromolecules, 253*(Pt 5), 127165, 127165.
Yang, Q.-Q., Farha, A. K., Kim, G., Gul, K., Gan, R.-Y., & Corke, H. (2020). Antimicrobial and anticancer applications and related mechanisms of curcumin-mediated photodynamic treatments. *Trends in Food Science & Technology, 97*, 341–354.
Yu, D.-G., Li, J.-J., Williams, G. R., & Zhao, M. (2018). Electrospun amorphous solid dispersions of poorly water-soluble drugs: A review. *Journal of Controlled Release, 292*, 91–110.
Yuan, Y., Huang, J., He, S., Ma, M., Wang, D., & Xu, Y. (2021). One-step self-assembly of curcumin-loaded zein/sophorolipid nanoparticles: Physicochemical stability, redispersibility, solubility and bioaccessibility. *Food & Function, 12*(13), 5719–5730.
Zhang, Z., Hu, Y., Ji, H., Lin, Q., Li, X., Sang, S., et al. (2023). Physicochemical stability, antioxidant activity, and antimicrobial activity of quercetin-loaded zein nanoparticles coated with dextrin-modified anionic polysaccharides. *Food Chemistry, 415*, Article 135736.
Zhi, K., Wang, R., Wei, J., Shan, Z., Shi, C., & Xia, X. (2021). Self-assembled micelles of dual-modified starch via hydroxypropylation and subsequent debranching with improved solubility and stability of curcumin. *Food Hydrocolloids, 118*, Article 106809.
Zhu, X., Chen, J., Hu, Y., Zhang, N., Fu, Y., & Chen, X. (2021). Tuning complexation of carboxymethyl cellulose/cationic chitosan to stabilize Pickering emulsion for curcumin encapsulation. *Food Hydrocolloids, 110*, Article 106135.